EXPERIMENTAL STUDY CONCERNING THE MOTION AND THE FRAGMENTATION OF LIQUID DROPLETS IN A GAS STREAM

E. V. Stekol'shchikov, M. P. Anisimova, I. A. Yatcheni, and O. L. Kondrat'ev

UDC 532.529.6

This study concerns the motion of single water drops with a diameter from 100 to 300 μ in a gradient stream of air with a maximum velocity up to 200 m/sec. Empirical relations are derived for the basic critical numbers characterizing the motion and the acceleration of droplets in an air stream, as functions of time.

Many studies have been concerned with the motion of particles in gas streams. In order to learn the scope of research on this subject, one needs only to look up the survey literature [1-4] with material on the motion of solid particles in a steady gas stream. Relatively few items have been published on the laws governing the motion of liquid (deformable) particles and this makes a generalization of results difficult.

During acceleration or deceleration of liquid particles by a gas stream there appear new physical phenomena which do not occur during interaction between such a stream and solid particles of another substance, namely a change in the aerodynamic shape of the droplet as a result of deformation, circulatory motion (Hill vortex) inside a droplet, and fragmentation of a single droplet.

There are generally many factors affecting the velocity and the acceleration of droplets. They include heat- and mass-transfer processes in the boundary layer of a droplet which result from evaporation, condensation, combustion, or chemical reactions, they also include an entire system of external forces: mass forces as those of gravity, magnetic, electrostatic, and similar forces, the Zhukovskii lift force, the force which carries a droplet due to turbulent fluctuations of the gas velocity, the forces due to thermophoresis, the aerodynamic drag forces in a steady (in relative motion) stream around a droplet, and the force due the gas-pressure gradient independently of the velocity gradient and the temperature gradient. One must also consider an entire set of transient effects, such as the inertial "coupling" of a gas mass to a droplet, the formation of boundary layers on the gaseous and on the liquid side, the development of a wake behind a droplet, the development of circulation inside a droplet, droplet deformations, the amplitude buildup of forced shape fluctuations, etc.

Nowhere in the published technical literature has the mechanism of droplet motion in a gas stream been analyzed to that full extent. Attention is usually focused on the individual aspects of this process. An overwhelming number of studies deals with the motion of a droplet deformed under steady conditions without internal circulation of the liquid or with a fully developed circulation [5-9]. In this study here the authors consider the motion of a droplet in a gradient stream of a gas.

The equation of a steady aerodynamic force carrying a particle

$$F_a = 0.5\,\psi k_m \left(\frac{\pi D^2}{4}\right) \rho_G (u_G - u_L)^2 \qquad (1)$$

will, when applied to a liquid droplet, be written in a form featuring fewer variables and an overall drag coefficient Π_ψ:

Moscow Institute of Power, Moscow. Translated from Inzhenerno-Fizicheskii Zhurnal, Vol. 23, No. 2, pp. 226-233, August, 1972. Original article submitted June 29, 1971.

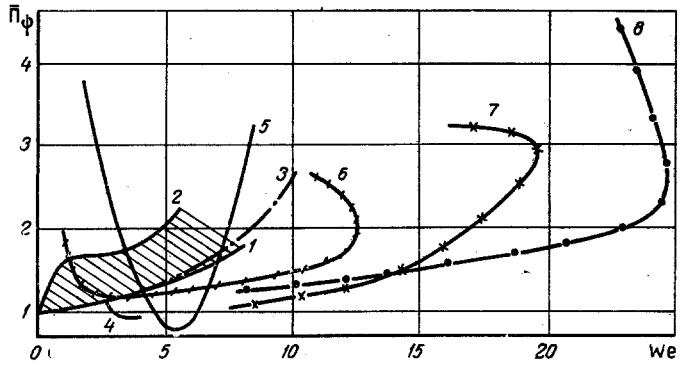

Fig. 1. Aerodynamic drag coefficient for liquid droplets, as a function of the Weber number: according to the test data in [6] (1, 2), according to the data in [5] (3), according to [7] (4), according to [17] (5), according to the results of this study with D = 0.186 mm and $\varepsilon = 0.95$ (6), with D = 0.104 mm and $\varepsilon = 0.814$ (7), and with D = 0.166 mm and $\varepsilon = 0.99$ (8).

$$F_a = \Pi_\psi \left(\frac{\pi D^2}{6} \right) \rho_G (u_G - u_L)^2. \tag{2}$$

In order to reveal any specific features of the aerodynamic drag mechanism which distinguish the behavior of liquid droplets from the behavior of solid spherical particles, we will introduce the parameters $\bar{\Pi}_\psi = \Pi_\psi / \Pi_\psi^S$. The shaded area between curves 1 and 2 in Fig. 1 indicates the range of possible qualitative and quantitative variations in the relative drag coefficient $\bar{\Pi}_\psi$, in the case of a liquid droplet, as a function of the Weber number. The region between curves 1 and 2 has been established on the basis of test results by various authors studying the fall of water droplets in air [6]. This region in Fig. 1 is characterized by the absence of liquid circulation inside a droplet. Moreover, the relative drag coefficient depends here on only one similarity criterion: the Weber number (the divergence of curves within the 1-2 region is explained by the measurement error. Relations (1) and (3) are considered the most reliable ones).

Often when the surface tension σ of a liquid is small and almost unaffected by surface-active substances, with a high circulation intensity developing in a droplet of a low-viscosity liquid in a steady stream, the Weber number is supplemented by another similarity criterion characterizing the effect of the intensity of internal circulation on the magnitude of parameter $\bar{\Pi}_\psi$. In the technical literature one finds the Morton number (Mo) or the Chao number (Ch) suggested [8]. The problem of finding the most appropriate oriental number for circulatory flow inside a droplet is still unresolved. To illustrate the significance of internal circulation in droplets of distilled water moving through air, in Fig. 1 is shown curve 4 based on an evaluation of the test data in [7]. Relation (4) corresponds to Ch = 0.84.

Within the range of "creeping" motion (Re < 1) the coefficient Π_ψ is determined from the Adamar–Rybchinskii relation [10]:

$$\bar{\Pi}_\psi = [2 + 3\Pi_\mu]/[3 + 3\Pi_\mu]. \tag{3}$$

For Re > 20 there are still no analytical relations for $\bar{\Pi}_\psi$ available sufficiently consistent with test results, which would account for the effect of steady deformation of a droplet with fully developed internal circulation.

The effect of transiency during the motion of solid spherical particles through air has been considered in [11]. Depending on the stream structure at the front surface of a poorly wetted body, one discerns three flow modes: 1) vortexfree flow (Stokes region); 2) flow with adjacent vortices; and 3) transient flow (Karman vortex trails). In a steady stream around a solid body during relative motion the intermode boundaries are fully determined by the Reynolds number [12, 13]. In a transient stream, where $\mu_G - \mu_L = f(\tau)$, the intermode boundaries are determined already not so much by the Reynolds number as by the Struhal number [9]. In studying the behavior of liquid droplets in transient gas streams, the authors of most published items were using the simplest form of the function $\mu_G - \mu_L = f(\tau)$ as a step function [14]. Such a mode of heavy loading was realized experimentally by a fast injection of a single droplet into a steady gas jet [15] or by placing a droplet in a gas stream behind a shock wave in stationary air [16]. An evaluation of the test data

Fig. 2. Operating segment of the test system. Operating substance: air sucked into the nozzle from the atmosphere. Maximum air velocity at the nozzle throat up to 200 m/sec. The last droplet on the right end of the chain of accelerated droplets is in the process of being fragmented.

in [16] yields at the initial values of the relative drag coefficient for a droplet at the beginning of the motion $\overline{\Pi}_\psi = 5\text{-}8$, at the maximum values of the Reynolds number $\mathrm{Re} \simeq 10^6$ and of the Weber number $\mathrm{We} \simeq 10^5$. Such high Reynolds and Weber numbers notwithstanding, the droplet at that instant has the shape of an oblate ellipsoid of revolution. When the droplet is in a highly transient stream, according to the results in [16], already neither the Reynolds number nor the Weber number govern the droplet acceleration. The complexity of the mechanism of droplet acceleration by a transient gas stream is further illustrated by relation (5) in Fig. 1, which has been obtained by an evaluation of the test data in [17] for intact water droplets 2 mm in diameter. According to relation (5), the drag coefficient for liquid droplets can, within a certain range of the Weber number, exceed appreciably the drag coefficient for these droplets in a steady stream. On the other hand, this drag coefficient can be smaller than the drag coefficient for solid spherical particles under otherwise the same conditions (in Fig. 1 this case corresponds to $\overline{\Pi}_\psi < 1$). In order to extend our knowledge about the variation of the coefficient Π_ψ and of other similarity criteria applicable to the motion of a droplet in a gas stream, appropriate experiments were performed at the Moscow Institute of Power. Distilled water from the condenser of a TÉTs turbine was the liquid substance. In order to reduce the number of measurable parameters, the effects of heat and mass transfer on the process of droplet acceleration were eliminated: air with a relative humidity approximately 90% was used as the continuous (carrier) medium. A Venturi tube with a rectangular cross section served as the accelerating device. The average variation of the air temperature in the tube was 9°C. The temperature of the liquid and the temperature of the gas were the same at the entrance to the accelerating segment. A chain of droplets with a given diameter was generated by a droplet generator operating on the principle of regularly breaking up a jet of liquid discharged from a capillary by periodic agitation [18].

In Fig. 2 is shown a photograph of an operating stage in the experiment. Unlike in most experimental studies, where the desired relations are established by the statistical method, the procedure here was to continuously observe the motion of just one droplet through a 50 mm long channel segment. The location of this droplet at various instants of time was tracked by means of high-speed kinematography in transmitted light, with the light source sufficiently far away from the plane of the film and together with the camera objective constituting a shadow system. Choosing the shadow-type optical system for high-speed kinematography contributed to a high resolving power in this method. A model CVDSh-500 arc lamp operating on dc current served as the light source. The film speed was 2000-10,000 frames/sec, the exposure time varied from 0.5 to 0.1 μsec/frame. On the basis of the kinematograms, relation $z = z(\tau)$ was determined for each specimen water droplet, whereupon its absolute velocity and acceleration were found by differentiating this curve. In Fig. 3 are shown the $z = z(\tau)$ curves for three specimen droplets. The monotonic trend of these curves indicates that the aerodynamic drag does not fluctuate, although theoretically this could happen as a result of either droplet shape fluctuations or of periodic vortex peeling in the trailing wake zone.

The evaluation of test data was based on the following equation of motion for droplets:

$$\left(1+\frac{s}{\Pi_\rho}\right)\frac{d\mathbf{u}_L}{d\tau}=\frac{\Pi_\psi|\mathbf{u}_G-\mathbf{u}_L|^2}{\Pi_\rho D}\,\mathbf{n}-\left(\frac{\zeta}{\rho_L}\right)\overrightarrow{\mathrm{grad}}\,p+\left(\frac{\Pi_\rho-1}{\Pi_\rho}\right)\mathbf{g}+\left(\frac{1+s}{\Pi_\rho}\right)\frac{d\mathbf{u}_G}{d\tau}+\frac{\mathbf{F}}{m}. \qquad (4)$$

The form factor is for a sphere $\zeta = 1$, for a thin disk $\zeta = 0$, and for a deformable liquid droplet $\zeta \leq 1$. Equation (4) is now multiplied by the vector $\mathbf{n}$, whereupon it yields the sought similarity complex Π_ψ:

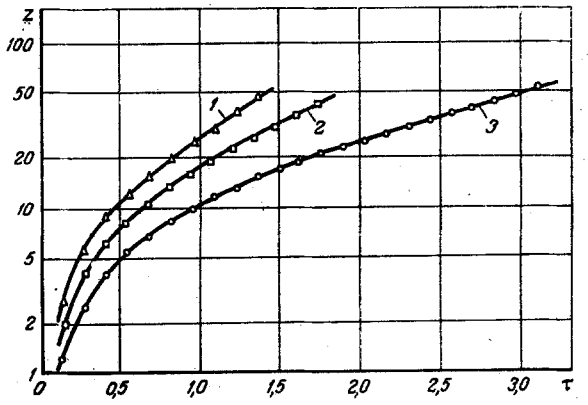

Fig. 3

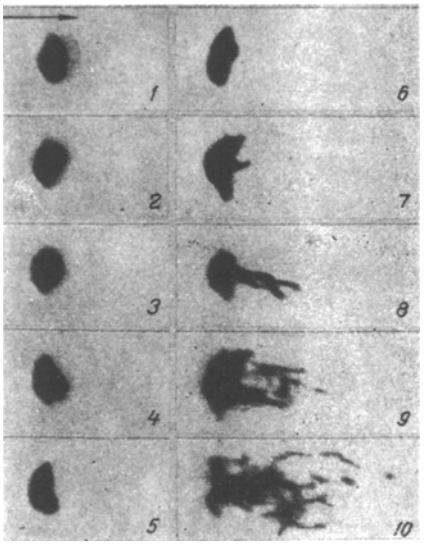

Fig. 4

Fig. 3. Path traversed by a droplet, as a function of time: 1) D = 0.104 mm; 2) 0.162; 3) 0.186.

Fig. 4. Stages of transient deformation of a droplet in a Venturi tube. D = 0.320 mm. Time interval between frames 0.13 μsec. Exposure of each frame 2 μsec. The arrow on frame 1 indicates the direction of motion of the droplet and the gas stream. Frame numbers 1-10.

$$\Pi_\psi = \Pi_\rho \Pi_a \left[1 + \frac{s}{\Pi_\rho} - \zeta \mathrm{Eu} - \left(\frac{1+s}{\Pi_\rho} \right) (\Pi_a)_G - \frac{\Pi_\rho - 1}{\Pi_\rho} \cdot \frac{1}{\mathrm{Fr}} - \mathrm{Ne} \right]. \tag{5}$$

The experiment for studying the motion of droplets was performed under the following conditions: **F** = 0 and **ng** = 0; the measurements yielded $\mathrm{Eu} < 10^{-3}$, $s < 2$, $\Pi_\rho > 835$, $\Pi_a < 1.6 \cdot 10^{-3}$, $(\Pi_a)_G < 38$. Considering the limitations realizable in the experiment, expression (5) could be greatly simplified to

$$\Pi_\psi = \Pi_\rho \Pi_a \left[1 - \left(\frac{1+s}{\Pi_\rho} \right) (\Pi_a)_G \right]. \tag{6}$$

On the basis of the Π-theorem in the similarity theory, we selected the following system of governing criteria: Sh, Π_0, Π_a, Π_μ, Lp, $(\Pi a)_G$, and We. Thus, the sought critical relation is of the form:

$$\nu = \nu(\mathrm{Sh}, \Pi_\rho, \Pi_a, \Pi_\mu, \mathrm{Lp}, (\Pi_a)_G, \mathrm{We}). \tag{7}$$

If necessary, one could use other systems of governing similarity criteria. The Lp, We, Π_ρ, Π_μ, Π_ψ, and ν numbers are related to the Reynolds number (Re), the Laplace number $(\mathrm{Lp})_L$ for the liquid phase, and the Stokes number (Stk) as follows:

$$\mathrm{Re} = \sqrt{\mathrm{Lp}\,\mathrm{We}}; \quad (\mathrm{Lp})_L = \frac{\Pi_\rho \mathrm{Lp}}{\Pi_\mu^2}; \quad \mathrm{Stk} = \frac{\Pi_\rho}{\Pi_\psi} \left(\frac{\nu}{1-\nu} \right)^2.$$

Time was measured from the instant the droplets passed through the control section. The largest relative errors of measurement were

$$\Delta u_G / u_G = 0.4\,\%; \quad \Delta u_L / u_L = 5\,\%; \quad \Delta D/D = 3.5\,\%; \quad \Delta \Pi_\psi / \Pi_\psi = 10\,\%.$$

An analysis of test data leads to conclusions concerning the feasibility of using them, at least partially, for a simulation of the process. The dependence of the relative drag coefficient $\overline{\Pi}_\psi$ on the Weber number, which has been found in this study, is shown in Fig. 1 (curves 6-8). Curves 6-8 have a few characteristic features. First of all, none of them lies within the range of steady noncirculatory deformation of droplets (within region 1-2). The slow increase in aerodynamic drag is due, first of all, to the development of circulation inside liquid droplets (each $\overline{\Pi}_\psi = f(\mathrm{We})$ curve has a minimum) and, secondly, to the

inertial lag of droplet deformation at values of the Weber number higher than at that minimum. The transient effects here are not related to the inertial "coupling" of masses or to the delay in the formation of an air boundary layer. At high values of the Weber number the trend of the $\overline{\Pi}_\psi = f(We)$ curves is "reciprocating." It is well known (e.g., [14]) that the shape of a droplet ceases to be stable at supercritical values of the Weber number. Moreover, the drag coefficient increases all the way until fragmentation of a droplet begins. This is always the case, even when both the Reynolds number and the Weber number decrease with time (diffusion zone in the Venturi tube). Curves 6-8 confirm this known fact. The trend of these curves is inseparably related to the stages of droplet deformation. Those latter are depicted in Fig. 4. Curves 6-8 in Fig. 1 indicate that, when droplets move through highly converging nozzles, the magnitude of the aerodynamic drag is appreciably affected by the time factor (Struhal number). In such situations the "steady-state" model for calculating the stream around a droplet cannot yield satisfactory results.

NOTATION

$D = (6V_L/\pi)^{1/3}$ is the equivalent diameter of a droplet;
f_m is the area of the median section;
g is the gravitational acceleration;
$k_m = f_m/(\pi D^2/4)$ is the median-section coefficient;
m is the mass of the droplet;
$Mo = (g\mu_G^4)/[\rho_G \sigma^3]$ is the Morton number;
p_{min} is the minimum static pressure in the Venturi tube;
p is the static pressure at any section of the tube;
p_0 is the total stagnation pressure at that section of the tube;
s is the mass coupling factor ($s = 0.5$ for a sphere, $s = 1.0$ for a cylinder in a transverse stream, etc.);
u_G, u_L are the velocities of gas and of liquid, respectively;
V_L is the volume of a droplet;
z is the linear coordinate;
$\Delta Sh = Sh - Sh_0$;
Sh_0 is the structural number at the first control section ($Sh_0 > 160$ in all cases);
$\varepsilon = p_{min}/p_0$;
μ_G, μ_L are the dynamic viscosities of gas and of liquid, respectively;
ρ_G, ρ_L are the densities of gas and of liquid, respectively;
$\Pi_\psi = 0.75\psi k_m$ is the aerodynamic drag parameter for a particle;
Π_ψ^s is the aerodynamic drag parameter for a solid sphere;
σ is the surface tension coefficient;
τ is the time;
ψ is the frontal drag coefficient for a particle;
ζ is the form factor of a particle;
$Ch = [2 + 3\Pi_\mu]/[1 + \sqrt{\Pi_\rho \Pi_\mu}]$ is the Chao number;
Stk is the Stokes number;
$\nu = u_L/u_G$ is the "slip" number;
$\mathbf{n} = (\mathbf{u}_G - \mathbf{u}_L)/|u_G - u_L|$ is the unit vector of relative velocity;
$\Pi_\rho = \rho_L/\rho_G$ is the density number;
$\pi_\mu = \mu_L/\mu_G$ is the viscosity number;
$Lp = (\rho_G D\sigma)/\mu_G^2$ is the Laplace number for the gaseous phase;
$(Lp)_L = (\rho_L D\sigma)/\mu_L^2$ is the Laplace number for the liquid phase;
$Sh = \frac{1}{D}\int_0^\tau (u_G - u_L)d\tau$ is the Struhal number;
$We = [\rho_G D(u_G - u_L)^2/\sigma]$ is the Weber number;
$Re = \rho_G D|u_G - u_L|/\mu_G$ is the Reynolds number;
F is the external force;
$\Pi_a = D(\mathbf{n}\,du_L/d\tau)/(u_G - u_L)^2$ is the acceleration number for a droplet;
$Eu = -(\mathbf{n}\,\overrightarrow{\text{grad}}\,p)/[\rho_L(\mathbf{n}\,du_L/d\tau)]$ is the Euler number;

$(\Pi_a)_G = (n\,du_G/d\tau)/(n\,du_L/d\tau)$ is the acceleration number for the gas;

$Fr = (n\,du_L/d\tau)/(ng)$ is the Froude number;

$Ne = (nF)/[m(n\,du_L/d\tau)]$ is the Newton number.

Subscripts

G denotes the gas;

L denotes the liquid (droplet).

LITERATURE CITED

1. N. A. Fuks, Mechanics of Aerosols [in Russian], Izd. AN SSSR, Moscow (1955).
2. N. A. Fuks, Progress in the Mechanics of Aerosols [in Russian], Izd. AN SSSR, Moscow (1961).
3. Z. R. Gorbis, Heat Transfer and Hydromechanics in Open Flow of a Dispersion [in Russian], Énergiya, Moscow (1970).
4. S. U. Soo, Dynamics of Multiple Systems, Waltham, Massachusetts, Toronto, London (1967).
5. B. V. Rauschenbach et al., Physical Principles of the Operating Process in the Combustion Chamber of Air-Reaction Engines [Russian translation], Mashinostroenie, Moscow (1964).
6. K. V. Beard and H. R. Pruppacher, J. Atmosph. Sci., 26, No. 5, Pt. 2, 1066 (1969).
7. J. L. Buzzard and R. M. Nedderman, Chem. Eng. Sci., 22, 1577 (1967).
8. S. Winikow and B. T. Chao, Phys. of Fluids, 9, No. 1, 50 (1966).
9. T. Sarpkaya and C. J. Garrison, Trans. ASME, 30E, No. 1, 19 (1963).
10. V. G. Levich, Physicochemical Hydrodynamics [in Russian], Fizmatgiz, Moscow (1959).
11. Selberg and Nicols, Rocket Engineering and Cosmonautics, 6, No. 3 (1968).
12. M. Van Dyke, Methods of Agitation in Fluid Mechanics [Russian translation], Mir, Moscow (1967).
13. G. Birkhof and E. Sarantonello, Jets, Wakes, and Cavities [Russian translation], Mir, Moscow (1961).
14. M. S. Volynskii and A. S. Lipatov, Inzh.-Fiz. Zh., 18, No. 5 (1970).
15. A. R. Hadson, E. G. Domich, and H. S. Adams, Phys. of Fluids, 6, No. 8, 1070 (1963).
16. Ranger and Nicols, Rocket Engineering and Cosmonautics, 7, No. 2 (1969).
17. B. P. Volgin and F. S. Yugai, Zh. Prikl. Mekh. Tekh. Fiz., No. 1 (1968).
18. Strom, Instr. for Sci. Res., No. 6 (1969).